

Controlled Growth and Cathodoluminescence Property of ZnS nanobelts with Large Aspect Ratio

Xiang Wu^{1, 2,*}, Ying Lei¹, Yufeng Zheng² and Fengyu Qu^{1,*}

ZnS nanobelts with large aspect ratio are successfully synthesized on a large scale through thermally evaporating of ZnS powder with a trace of SnO₂ powder using gold coated Si wafer as the substrate at 1100°C. The results indicate that the as-obtained ZnS nanobelts are about 10 nm in thickness and hundreds of micrometers in length, and the aspect ratio reaches more than 10⁴. Substrate dependent experiments are conducted to better study the growth mechanism of the ZnS nanobelts. Subsequently, optical properties of the as-synthesized ZnS nanobelts are also investigated by using a cathodoluminescence (CL) system, which shows the existence of a strong ultraviolet emission at 342 nm and two poor emission peaks at 522 nm and 683 nm at room temperature, respectively.

Keywords: Semiconductor; ZnS; Nanobelts; Cathodoluminescence

Citation: Xiang Wu, Ying lei, Yufeng Zheng and Fengyu Qu, "Controlled Growth and Cathodoluminescence Property of ZnS Nanobelts with Large Aspect Ratio", Nano-Micro Lett. 2, 272-276 (2010). [doi:10.3786/nml.v2i4.p272-276](https://doi.org/10.3786/nml.v2i4.p272-276)

Different from the geometry shapes of the nanorod, nanowire and nanotube, the nanobelt possesses a rectangle-like cross section with large width-to-thickness ratio and high aspect ratio. Nanobelts of different components with various morphologies have been synthesized, including elements [1, 2], oxides [3, 4], nitrides [5], sulfides [6-11] even ternary compounds [12, 13] since Pan et al. first reported the formation of nanobelts of semiconductor oxides in 2001 [14]. With the special geometry shapes and microstructure, the belt-like nanostructures have been the research focus due to their unique physical and chemical properties, such as optical [15, 16], electrical [17] and sensor [18, 19], field emission [20, 21], optoelectronic properties [22-24], and so on. Therefore, it is important to obtain the desiring nanobelts with uniform dimensions and sizes and controllable structures for the integration of nanodevices based nanobelt building blocks.

As an important semiconductor compound material, ZnS with a direct wide band gap (3.68 eV) and exciton binding energy of 40 meV at room temperature, has a high refractive index and a high transmittance in the visible range [25]. Many efforts have been made on synthesis of one dimensional (1D)

ZnS nanobelts in recent years by a variety of methods. Zhang et al. reported bicrystal ZnS nanobelts through a chemical vaporation method on Si and KCl substrates, respectively [26]. Meng et al synthesized dart-shaped tricrystal ZnS nanoribbons by simple thermal evaporation of the mixture of ZnS and SiO and studied the growth mechanism in detail [27]. Hao et al. investigated the growth of periodically twinned nanobelts of ZnS and thought the mass diffusion played an important role in the growth process of the twinned ZnS nanobelts [28]. Fang et al. synthesized ultrafine ZnS nanobelts as good field emitters [21]. Herein, we successfully fabricated ZnS nanobelts with large aspect ratio by adjusting the substrate types and the evaporation rate, and studied the CL properties of the as-obtained products. ZnS nanobelts reported here are good candidates for optical and optoelectronic devices.

ZnS nanobelts with large aspect ratio were synthesized through a thermal evaporation process in a horizontal tube furnace with Au catalyst on Si substrate. A Si wafer (1 cm in length and 5 mm in width) was placed downstream, which is 20 cm away from the source material. 1 g commercial-grade ZnS powder with 0.2 g SnO₂ was placed in the center of a

¹College of Chemistry and Chemical Engineering, Harbin Normal University, Harbin 150025, P. R. China

²Center for Biomedical Materials and Engineering, Harbin Engineering University Harbin 150001 P. R. China

*Corresponding author. E-mail: wuxiang05@gmail.com; qufengyu@hrbnu.edu.cn

single-zone tube furnace and evacuated for 2 hours to purge oxygen from the chamber, then the furnace was heated to 1100°C at a rate of 20 °C /min and keep at this temperature for 1h. A carrier gas of high-purity Ar was kept flowing at a rate of 50 sccm. The pressure inside the tube was maintained at 300 Torr during the whole experiment. After the furnace was cooled to room temperature, a gray wool-like product was deposited on Si substrate. A series of control experiments were conducted by changing the substrate types. The collected products were characterized by a scanning electron microscope (SEM, Hitachi S-4800) equipped with an energy-dispersive X-ray detector (EDX, INCA300), and a transmission electron microscope (JEOL JEM-3010). Cathodoluminescence properties are investigated by means of a thermal field emission scanning electron microscope (Hitachi S4200) equipped with a CL system. The CL spectra and images are taken at room temperature at 5 kV and 70 pA.

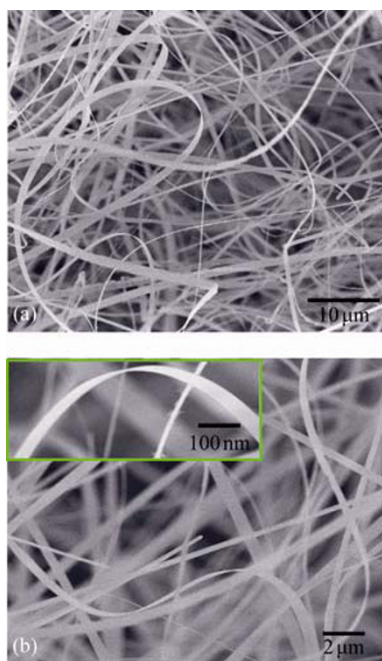


FIG. 1. SEM images of the as-obtained ZnS nanobelts (a) General SEM image of the as-synthesized product; (b) High magnification SEM image, the inset is a local SEM image of ZnS nanobelt.

Figure 1 shows SEM images of the as-grown ZnS nanobelts. A low magnification SEM image in Fig. 1(a) indicates the nanobelts are tens of micrometers in length. Fig. 1(b) is a high magnification SEM image, indicating a good bending characteristic of the nanobelt. Each nanobelt has a uniform width along the entire length direction; the inset in Fig. 1(b) is a local SEM image, showing clearly the thickness of only about 10 nm. A typical XRD pattern from the as-grown product is shown in Fig. 2(a), where all the diffraction peaks can be indexed to wurzite structured ZnS with lattice constants of

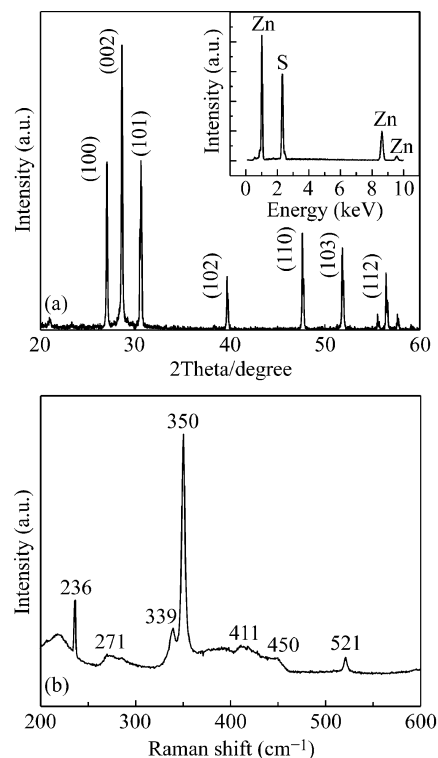


FIG. 2. (a) Raman spectrum of the as-synthesized ZnS nanobelts (b) XRD pattern of as-synthesized ZnS nanobelts.

$a=0.382$ nm and $c=0.625$ nm (PCPDS card: 36-1450), no SnO_2 peaks are found, which means the as-synthesized ZnS nanobelt has a high purity. The inset in Fig. 2(a) is an EDS spectrum, which is consistent with the XRD pattern result. Raman spectrum from the as-grown nanobelts is shown in Fig. 2(b) the much weaker peak at 521 cm^{-1} is from Si substrate. The dominate spectrum is 350 cm^{-1} , which is designated as longitudinal optical (LO) phonon mode. The weaker peak at 271 cm^{-1} is associated with transverse optical (TO) phonon mode. Some phonon peaks by these selection rules will become stronger in a particular scattering geometry due to all of nanobelts grown along the same direction, the same as that of the wires reported by Lin et al [29]. Besides the characteristic peaks, Raman peaks located at 236, 339, 411 and 450 cm^{-1} are also observed, which can be attributed to plasmon-enhanced resonant Raman effect [30].

TEM is used to further study the microstructures of the as-grown ZnS nanobelts. Figures 3(a) and 3(b) show low magnification TEM and HRTEM images, respectively. The HRTEM image reveals the nanobelts of ZnS are structurally uniform. The measured spacing of 0.626 nm corresponds to the distance between (001) plane of the ZnS nanobelts. The inset in Fig. 3(b) is the selected area electron diffraction (SAED) pattern

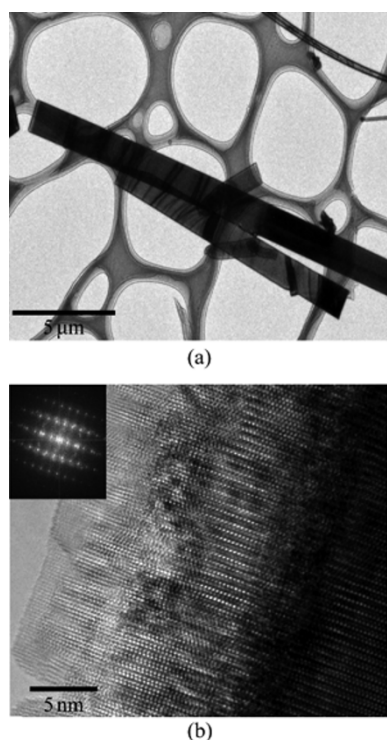


FIG. 3. TEM images of the as-obtained ZnS nanobelts (a) Low magnification TEM image; (b) HRTEM image, the inset is the corresponding SAED pattern.

of the as-grown ZnS nanobelt, confirming that the as-grown ZnS nanobelt is single crystal and grows along [001] direction.

To better investigate the formation of ZnS nanobelts with large aspect ratio, substrate dependent comparison experiments were conducted. When using tungsten thread as the deposition substrate, the beltlike structured ZnS still exist, but the thickness is about 100 nm, as shown in Fig. 4(a). When tungsten wafer substitutes for tungsten thread as the substrate (see Figure 4(b)),

the thickness of ZnS nanobelts are larger and their length became shorter. The inset in Fig. 4(b) is the local enlarged SEM image; one can see the thickness is about 300 nm. The phenomenon indicates that though the same type substrate, different surface of the substrate (smooth or curved) have crucial effect on the size and dimension of the as-obtained ZnS product.

Due to using gold coated Si wafer as the substrate, ZnS nanobelts with large aspect ratio can be formed. Otherwise, only large scale ZnS nanorod arrays are formed when using bare silicon wafer as the substrate, as shown in Fig. 4(c) and 4(d), which indicate that gold catalyst play an important role in the growth of ZnS nanobelts with large aspect ratio. Therefore, the growth of ZnS nanobelt with large aspect ratio is dominated by vapor-liquid-solid (VLS) mechanism [31]. At first, ZnS powder evaporates into Zn vapor and sulfur vapor at high temperature. As the reaction proceeds, Zinc vapor diffuses and meets the sulfur vapor together with the carrier gas and dissolve into liquid gold catalyst and form a small liquid droplet. ZnS crystals shall precipitates from solid-liquid interface with the favorite growth direction when the concentration of Zn and S atoms in the droplet is greater than the saturation. No gold nanoparticles were found here, it is possible that the Au particle catalysts have been evaporated when the growth of the ZnS nanobelts finishes, which is consistent with the explanation to the growth of ZnO nanowires and nanohelices [32, 33]. Previously we reported the synthesis of fishbonelike ZnS nanostructures through using ITO glass as the substrate [34]. It shows that each substrate has

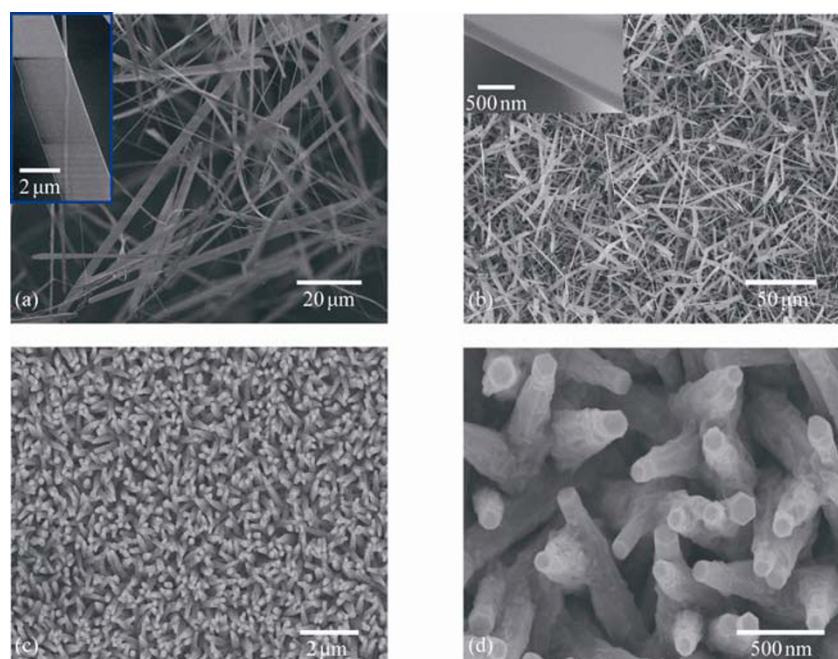


FIG. 4. SEM images of the as-synthesized products in the different substrates (a) Tungsten thread; (b) Tungsten wafer; (c-d) silicon wafer.

different interface with the as-grown ZnS nanostructures, which determines the nucleation rates of the nanoparticles and then the final morphologies of the as-obtained product. Therefore, in synthesizing the nanostructures by thermal evaporation method, besides considering growth temperature [35, 36], choosing the suitable deposition substrate is also important for getting the desired nanostructures for future micro/nanodevices integration.

There are many reports about photoluminescence and cathodoluminescence of semiconductor nanostructures [37-40]. Cathodoluminescence measurement of ZnS nanobelts with large aspect ratio was conducted at room temperature at 5 kV and 70 pA. CL spectrum of the as-synthesized ultrathin ZnS nanobelts is showed in Figure 5, where there are three emission peaks at 342 nm, 522 nm and 683 nm, respectively. The stronger emission peak at 342 nm can be ascribed to intrinsic characteristic emission. Due to quantum effect there is a slight shift of 5 nm, comparing to bulk ZnS powder. About the peak at 522 nm, Liu et al. studied the Cd-doped ZnS nanostructures and attributed it to Cd doping [41]. Xu et al. have observed a green emission band at 507 nm in Cu-doped ZnS nanocrystals [42]. Liang et al proposed it is likely related to the gold impurity induced deep level emission [43]. In the present experiment, gold was also employed as catalyst. Therefore the green emission at 522 nm can be attributed to gold impurity. The origin of the red light emission about ZnS nanostructures is seldom explained, Liu et al studied Cd and Mn co-doped ZnS nanostructures and thought the red light emission originated from the interaction of Mn and Cd pairs. This emission could be strengthened by adjusting the Mn and Cd content in ZnS [44]. In our work, no Cd or Mn doping, therefore it is no the case for the reported ZnS nanobelts here. We propose the emission perhaps happen during electron transit from oxygen vacancy to valence band due to a trace of

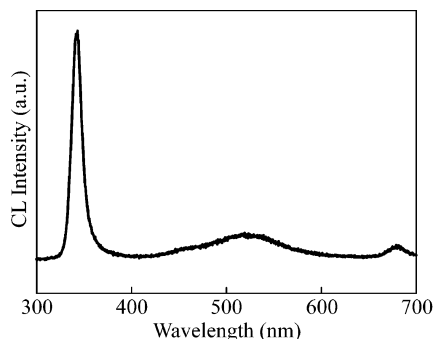


FIG. 5. CL spectrum of the as-obtained ZnS nanobelts.

the addition of Sn element. More systematic studies shall be conducted to full understand the origin of this emission band and shall be reported elsewhere.

In summary, ZnS nanobelts with large aspect ratio have been synthesized by using gold coated Si wafer as the substrate. The as-grown ZnS nanobelts with high width-thickness ratio are about 10 nm in thickness and tens of micrometers in length. Substrate types play the important roles in determining the size and thickness of the as-obtained products. Gold mediated VLS process is responsible for the nucleation and growth of the ZnS nanobelts with large aspect ratio. CL spectrum shows that there are a stronger ultraviolet emission peak at 342 nm and two poor visual peaks at 522 nm and 683 nm.

This work was sponsored by the Scientific Research Fund of Heilongjiang Provincial Education Department (11551117) and China Postdoctoral Foundation (20090460875), Pre-research Fund (2009KYG-01) and Youth Skeleton Teacher Fund (10KXQ-07) of Harbin Normal University. We thank Dr. Kentaro Watanabe for his kind help in CL test.

References

1. A. M. Qin, Z. Li, R. S. Yang, Y. D. Gu, Y. Z. Liu and Z. L. Wang, *Solid Stat. Commun.* 148, 145 (2008). [doi:10.1016/j.ssc.2008.07.039](https://doi.org/10.1016/j.ssc.2008.07.039)
2. D. P. Wang and Q. Chen, *J Phys. Chem. C* 112, 15129 (2008).
3. Z. R. Dai, Z. W. Pan and Z. L. Wang, *Adv. Funct. Mater.* 13, 9 (2003). [doi:10.1002/adfm.200390013](https://doi.org/10.1002/adfm.200390013)
4. L. Zhang, X. Yang, J. Dong and Y. Xie, *Chem. Mater.* 21, 5681 (2009). [doi:10.1021/cm9023887](https://doi.org/10.1021/cm9023887)
5. H. B. Zeng, C. Y. Zhi, Z. H. Zhang, X. L. Wei, X. B. Wang, W. L. Guo, Y. Bando and D. Golberg, *Nano Lett.* 10, 5049 (2010). [doi:10.1021/nl103251m](https://doi.org/10.1021/nl103251m)
6. L. Li, P. S. Lee, C. Y. Yan, T. Y. Zhai, X. S. Fang, M. Y. Liao, Y. Koide, Y. Bando and D. Golberg, *Adv. Mater.* 22, 5145(2010). [doi:10.1002/adma.201002608](https://doi.org/10.1002/adma.201002608)
7. F. Lu, W. P. Cai, Y. G. Zhang, Y. Li, F. Q. Sun, S. H. Seo and S. O. Cho, *J Phys. Chem. C* 111, 13385 (2007).
8. L. Li, X. S. Fang, T. Y. Zhai, M. Y. Liao, U. K. Gautam, X. C. Wu, Y. Koide, Y. Bando and D. Golberg, *Adv. Mater.* 22, 4151 (2010). [doi:10.1002/adma.201001413](https://doi.org/10.1002/adma.201001413)
9. X. C. Wu, Y. R. Tao and Q. X. Gao, *Nano Res.* 2, 558 (2009). [doi:10.1007/s12274-009-9055-2](https://doi.org/10.1007/s12274-009-9055-2)
10. P. C. Wu, R. M. Ma, C. Liu, T. Sun, Y. Ye and L. Dai, *J Mater. Chem.* 15, 2125 (2009). [doi:10.1039/b822518d](https://doi.org/10.1039/b822518d)
11. L. Li, P. C. Wu, X. S. Fang, T. Y. Zhai, L. Dai, M. Y. Liao, Y. Koide, H. Q. Wang, Y. Bando and D. Golberg, *Adv. Mater.* 22, 3161(2010). [doi:10.1002/adma.201000144](https://doi.org/10.1002/adma.201000144)

12. Y. Su, S. Li, L. Xu, Y. Q. Chen, Q. T. Zhou, B. Peng, S. Yin, X. Meng, X. M. Liang and Y. Feng, *Nanotechnology* 17, 6007 (2006). [doi:10.1088/0957-4484/17/24/017](https://doi.org/10.1088/0957-4484/17/24/017)
13. Y. Li and X. L. Ma, *Phys. Stat. Sol. A* 202, 435 (2005). [doi:10.1002/pssa.200406924](https://doi.org/10.1002/pssa.200406924)
14. Z. W. Pan, Z. R. Dai and Z. L. Wang, *Science* 291, 1947 (2001). [doi:10.1126/science.1058120](https://doi.org/10.1126/science.1058120)
15. G. Z. Shen, D. Chen, P. C. Chen and C. W. Zhou, *ACS Nano* 3, 1115 (2009). [doi:10.1021/nn900133f](https://doi.org/10.1021/nn900133f)
16. Z. Fang, K. B. Tang, J. M. Shen, G. Z. Shen and Q. Yang, *Cryst. Growth Des.* 7, 2254 (2007). [doi:10.1021/cg0607755](https://doi.org/10.1021/cg0607755)
17. J. Lin, Y. Huang, Y. Bando, C. C. Tang, C. Li and D. Golberg, *ACS Nano* 4, 2452 (2010). [doi:10.1021/nn100254f](https://doi.org/10.1021/nn100254f)
18. Y. G. Li, P. Feng, X. Y. Xue, S. L. Shi, X. Q. Fu, C. Wang, Y. G. Wang and T. H. Wang, *Appl. Phys. Lett.* 90, 042109 (2007). [doi:10.1063/1.2432278](https://doi.org/10.1063/1.2432278)
19. E. Comini, G. Faglia, G. Sberveglieri, Z. W. Pan and Z. L. Wang, *Appl. Phys. Lett.* 81, 1869 (2002). [doi:10.1063/1.1504867](https://doi.org/10.1063/1.1504867)
20. H. Zhang, W. Q. Ding, K. He and M. Li, *Nanoscale Res. Lett.* 5, 1264 (2010). [doi:10.1007/s11671-010-9635-9](https://doi.org/10.1007/s11671-010-9635-9)
21. X. S. Fang, Y. Bando, G. Z. Shen, C. H. Ye, U. K. Gautam, P. M. F. J. Costa, C. Y. Zhi, C. C. Tang and D. Golberg, *Adv. Mater.* 19, 2593 (2007). [doi:10.1002/adma.200700078](https://doi.org/10.1002/adma.200700078)
22. X. S. Fang, S. L. Xiong, T. Y. Zhai, Y. Bando, M. Y. Liao, U. K. Gautam, Y. Koide, X. G. Zhang, Y. T. Qian and D. Golberg, *Adv. Mater.* 21, 5016 (2009). [doi:10.1002/adma.200902126](https://doi.org/10.1002/adma.200902126)
23. C. S. Lao, Y. Li, C. P. Wong and Z. L. Wang, *Nano Lett.* 7, 1323 (2007). [doi:10.1021/nl070359m](https://doi.org/10.1021/nl070359m)
24. J. H. He, Y. H. Lin, M. E. Mcconney, W. Tsukruk, Z. L. Wang and G. Bao, *J Appl. Phys.* 102, 084303 (2007). [doi:10.1063/1.2798390](https://doi.org/10.1063/1.2798390)
25. S. Yamaga, A. Yoshikawa and H. Kasai, *J. Cryst. Growth* 86, 252 (1998). [doi:10.1016/0022-0248\(90\)90725-Z](https://doi.org/10.1016/0022-0248(90)90725-Z)
26. Z. X. Zhang, J. X. Wang, H. J. Yuan, Y. Gao, D. F. Liu, L. Song, Y. J. Xiang, X. W. Zhao, L. F. Liu, S. D. Luo, X. Y. Dou, S. C. Mou, W. Y. Zhou and S. S. Xie, *J. Phys. Chem. B* 109, 18352 (2005). [doi:10.1021/jp052199d](https://doi.org/10.1021/jp052199d)
27. X. Fan, X. M. Meng, X. H. Zhang, W. S. Shi, W. J. Zhang, J. A. Zapien, C. S. Lee and S. T. Lee, *Angew. Chem. Int. Ed.* 45, 2568 (2006). [doi:10.1002/anie.200504069](https://doi.org/10.1002/anie.200504069)
28. Y. F. Hao, G. W. Meng, Z. L. Wang, C. H. Ye and L. D. Zhang, *Nano Lett.* 6, 1650 (2006). [doi:10.1021/nl060695n](https://doi.org/10.1021/nl060695n)
29. M. Lin, T. Sudhiranjan, C. Boothroyd and K. P. Loh, *Chem. Phys. Lett.* 400, 175 (2004). [doi:10.1016/j.cplett.2004.10.115](https://doi.org/10.1016/j.cplett.2004.10.115)
30. M. Abdulkhadar and B. thomas, *Nanostruc. Mater.* 5, 289 (1995). [doi:10.1016/0965-9773\(95\)00237-9](https://doi.org/10.1016/0965-9773(95)00237-9)
31. R. S. Wagner and W. C. Ellis, *Appl. Phys. Lett.* 4, 89 (1964). [doi:10.1063/1.1753975](https://doi.org/10.1063/1.1753975)
32. S. Bae, J. Lee, H. Jung, J. Park and J. Ahn, *J. Am. Chem. Soc.* 127, 10802 (2005). [doi:10.1021/ja0534102](https://doi.org/10.1021/ja0534102)
33. X. Wu, W. Cai and F. Y. Qu, *Chin. Phys. B* 18, 1669 (2009). [doi:10.1088/1674-1056/18/4/065](https://doi.org/10.1088/1674-1056/18/4/065)
34. X. Wu, F. Y. Qu, G. Z. Shen and W. Cai, *J. Alloys Compd.* 482, L32 (2009). [doi:10.1016/j.jallcom.2009.04.070](https://doi.org/10.1016/j.jallcom.2009.04.070)
35. X. S. Fang, C. H. Ye, L. D. Zhang, Y. H. Wang and Y. C. Wu, *Adv. Funct. Mater.* 15, 63 (2005). [doi:10.1002/adfm.200305008](https://doi.org/10.1002/adfm.200305008)
36. X. Wu, J. H. Sui, W. Cai and P. Jiang, *Chin. Phys. Lett.* 25, 737 (2008). [doi:10.1088/0256-307X/25/2/104](https://doi.org/10.1088/0256-307X/25/2/104)
37. H. B. Zeng, G. T. Duan, Y. Li, S. K. Yang, X. X. Xu and W. P. Cai, *Adv. Funct. Mater.* 20, 561(2010). [doi:10.1002/dfm.200901884](https://doi.org/10.1002/dfm.200901884)
38. H. B. Chen, X. Wu, L. H. Gong, C. Ye, F. Y. Qu and G. Z. Shen, *Nanoscale Res. Lett.* 5, 570 (2010). [doi:10.1007/11671-009-9506-4](https://doi.org/10.1007/11671-009-9506-4)
39. Y. T. Han, X. Wu, G. Z. Shen, B. Dierre, L. H. Gong, F. Y. Qu, Y. Bando, T. Sekiguchi, F. Fabbri and D. Golberg, *J. Phys. Chem. C* 114, 8235(2010). [doi:10.1021/jp100942m](https://doi.org/10.1021/jp100942m)
40. H. B. Zeng, W. P. Cai, Y. Li, J. L. Hu and P. S. Liu, *J. Phys. Chem. B* 109, 18260(2005). [doi:10.1021/jp052258n](https://doi.org/10.1021/jp052258n)
41. J. Z. Liu, P. X. Yan, G. H. Yue, J. B. Chang, D. M. Qu and R. F. Zhuo, *J. Phys. D: Appl. Phys.* 39, 2352 (2006).
42. S. J. Xu, S. J. Chua, B. Liu, L. M. Gan, C. H. Chew and G. Q. Xu, *Appl. Phys. Lett.* 73, 478(1998). [doi:10.1063/1.121906](https://doi.org/10.1063/1.121906)
43. H. Liang, Y. Shimizu, T. Sasaki, H. Umehara and N. Koshizaki, *J. Phys. Chem. B* 108, 9728 (2004). [doi:10.1021/p037963f](https://doi.org/10.1021/p037963f)
44. J. Z. Liu, P. X. Yan, G. H. Yue, J. B. Chang, D. M. Qu and R. F. Zhuo, *J. Phys. D: Appl. Phys.* 39, 2352(2006). [doi:10.1088/0022-3727/39/11/006](https://doi.org/10.1088/0022-3727/39/11/006)